MULTILEVEL ADAPTIVE MESH MODELING FOR WAVE PROPAGATION IN LAYER MEDIA

TIELIANG MI[1], JIANWEI MA[1,2], HERVÉ CHAURIS[2] and HUIZHU YANG[1]

[1] *Institute of Seismic Exploration, School of Aerospace, Tsinghua University, Beijing 100084, China.*
[2] *Center of Geoscience, Mines ParisTech, 35 rue Saint-Honoré, 77300 Fontainebleau, France. herve.chauris@mines-paristech.fr*

(Received April 30, 2009; revised version accepted September 8, 2009)

ABSTRACT

Mi, T., Ma, J., Chauris, H. and Yang, H., 2010. Multilevel adaptive mesh modeling for wave propagation in layer media. *Journal of Seismic Exploration*, 19: 121-139.

In this paper, we apply an adaptive mesh refinement method for numerical modeling of two-dimensional wave propagation in blocky models. A blocky model consists of patches with homogeneous properties. A series of nested-type adaptive meshes of local rectangular finer or finest mesh patches is used to control the solution accuracy at each level. The high-resolution simulation of wave propagation can be obtained effectively from coarser mesh to finer mesh level. Numerical experiments show good performance of the proposed algorithm to obtain fine characteristics of wave propagation (in particular reflected, transmitted, diffracted energy) while avoiding numerical dispersion.

KEYWORDS: adaptive mesh refinement, wave propagation, high-resolution algorithm, absorbing boundary conditions.

INTRODUCTION

Many different numerical methods have been developed to simulate wave propagation in the field of seismic exploration. The most commonly used methods are finite difference, finite element and spectral methods. The finite difference methods may suffer from numerical dispersion for a too large grid space step. The finite element methods require larger memory storage.

0963-0651/10/$5.00

Pseudo-spectral methods are of relatively high accuracy but are more computationally intensive. These methods have respective shortcoming that do not satisfy at the same time the requirements of highly accurate and efficient simulation of wave propagation. In order to obtain more effective numerical modeling methods, we apply the adaptive mesh refinement (AMR) algorithm for modeling the wave propagation in some specific models.

Wave propagation is modeled in the earth's interior that has large scale features and discontinued solutions. The structure of the earth is usually unknown and has to be determined through an inversion process such as traveltime tomography. In a given velocity model, computed travel times are compared to the observed traveltimes picked on seismograms (Bishop et al., 1986). Because of limited illumination, the inversion scheme is not well determined and one needs to impose some constraints during the minimization process or to reduce the number of unknown velocity parameters. Typically, the earth is described by blocky models, consisting of adjacent zones with homogeneous properties. The boundaries between blocks can however be complex. In this context, AMR dynamically adapts numerical techniques for solving partial differential equations (PDE) by using variable space and time steps depending on the local error of solutions in different computational domains. As a starting point, the AMR algorithm computes a solution on a coarse grid covering the entire domain. The fine grids, usually rectangular Cartesian subgrids, are adaptively nested in patches on the coarse grid. Finer subgrids are recursively added until a given optimal level is reached for the local truncation error. The solution of local fine regions automatically updates the corresponding solution on the coarse grid. The AMR algorithm thus provides a framework, in which different numerical simulations can be applied in different regions and at different levels to represent the wave propagation.

The original motivation of applying AMR algorithm to finite difference schemes was first proposed by Berger (1982). Berger and Oliger (1984) presented the adaptive mesh refinement method for the solution of the systems of hyperbolic PDEs using finite difference methods in two dimensions based on multilevel adaptive grids. Bolstad (1982) used an AMR finite difference algorithm for an initial boundary value problem in the case of one-dimensional hyperbolic problems. Berger and Colella (1989) developed an automatic adaptive mesh refinement for applications for solving shock hydrodynamics in two spatial dimensions. Berger and LeVeque (1998) described a more general framework that employed high-resolution wave propagation algorithms with adaptive mesh refinement for hyperbolic systems. Barad and Colella (2005) presented a block-structured local refinement solution for Poisson's equation based on conservative law to obtain a fourth-order accuracy. Qian and Symes (2002) used adaptive upwind finite difference methods for the paraxial eikonal equation based on a posterior error estimation to control automatic grid refinement generation. Griebel and Zumbusch (1998) used adaptive sparse grid

discretization techniques for the numerical solution of scalar hyperbolic conservation laws. Trangenstein (1995) extended the two-dimensional AMR algorithm for solid dynamics with more elaborate refluxing steps. Pancheshnyi et al. (2008) used AMR algorithm for the continuity equations and 2D and 3D Poisson's equation with high-order finite volume discretization. Mi et al. (2009) used second-generation wavelets as a tool that controls errors to structure multilevel adaptive grids to solve for the wave equation. One of main advantages of these adaptive methods is that one does not need to replicate fine mesh storage at every time and automatically generate adaptive mesh. So far, the AMR method is a good tool for computational solutions, but still new for application related to or seismic wave propagation.

When solving the wave propagation in large scale, we need to define adequate fine grids. If the same fine grid is used for the entire domain, this could lead to very expensive numerical schemes, because many regions do not need high levels of refinement grid. AMR algorithm allows local rectangular fine grids where it is needed, to obtain better resolution of wave propagation. In this paper, we apply the AMR method and high-resolution wave propagation

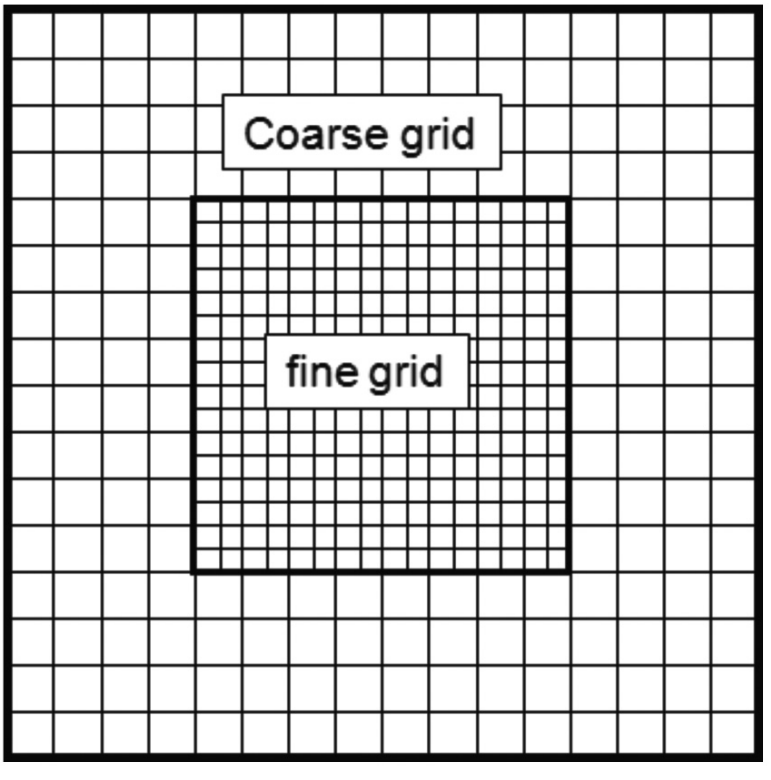

Fig. 1. Adaptive mesh refinement with local rectangular grid.

algorithms for the simulation of wave propagation, in order to obtain more accurate and high resolution solution for the wave equation. We focus on the characteristics of wave propagation in the blocky models.

DATA STRUCTURE FOR AMR

In the two-dimensional spatial domain, the representations of data structures are more complex than for the one-dimensional case. The AMR starts from a rectangular coarse grid denoted by G_0. $G_{0,1}$ is part of G_0 with the same mesh space steps $h_x = h_y = h$ on all components at level 0. If a region, e.g., $G_{1,0}$ needs some refinement, we generate a set of local rectangular finer subgrids $\{G_{1,1},G_{1,2},G_{1,3},G_{1,4}\}$ having the same mesh space steps h/2 at level 1. Next, $G_{1,1}$ generates a finer subgrids $G_{2,1}$, and $G_{2,1}$ generates a finer subgrids $G_{2,2}$, $G_{1,3}$ has two finer subgrids $G_{2,3}$ and $G_{2,4}$, $G_{1,4}$ generates a finer subgrids $G_{2,5}$, where all the finer subgrids $\{G_{2,1},G_{2,2},G_{2,3},G_{2,4},G_{2,5}\}$ have the same mesh space steps h/4 at level 2 [see Fig. 2(a)]. All local rectangular finer subgrids are nested within coarse grid $G_{0,1}$ covering the corresponding regions. The coarsest level mesh covers the entire computational domain and each finer level mesh covers a portion of the interior of the next fine level mesh (Berger, 1986; Berger and Rigoutsos, 1991). In this way, a nested sequence of grids with finer and finer discretizations till a given level of accuracy is satisfied. The finer meshes have the same spatial width in each level, and the neighbour level meshes are refined by a ratio of 2:1.

The data structure of the AMR algorithm is a tree structure where each grid at every level corresponds to a node in the tree. If a finer grid is nested in a coarse grid, it is said that the corresponding node in the tree is an offspring of the parent node for the coarse grid. At the same level, finer grids are called siblings, if they do not have the same parents called neighbors indicated by the dashed lines [see Fig. 2(b)] (Berger, 1986; Berger and Rigoutsos, 1991; Mitra et al., 1997). Each node is defined a fixed number of lists of information describing the grid on the tree data structure.

If the level allows refinement, then it is necessary to make sure that the number of time steps will be a multiple of the finer mesh interval. However, we do not assume that a successful time step on the upper level can be divided by the spatial refinement ratio to provide a successful time step on the finer level. We need to check all grid cells at every time steps to determine whether these regions are needed for refinement. AMR refines in time and space at each level. In other words, space steps and time steps both have the same mesh refinement ratio r (see Fig. 3) (Debreu et al., 2008; Horning and Trangenstein, 1997). By definition, the space mesh refinement ratio is $r = dx_{l-1}/dx_l$, and the time refinement ratio is $r = dt_{l-1}/dt_l$. Thus, $dt_l/dx_l = dt_{l-1}/dx_{l-1} = \cdots dt_1/dx_1 =$ constant, where l denotes the level of refinement.

(a)

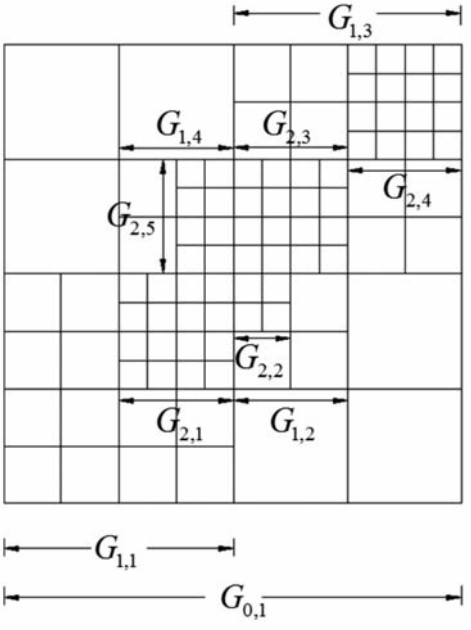

(b)

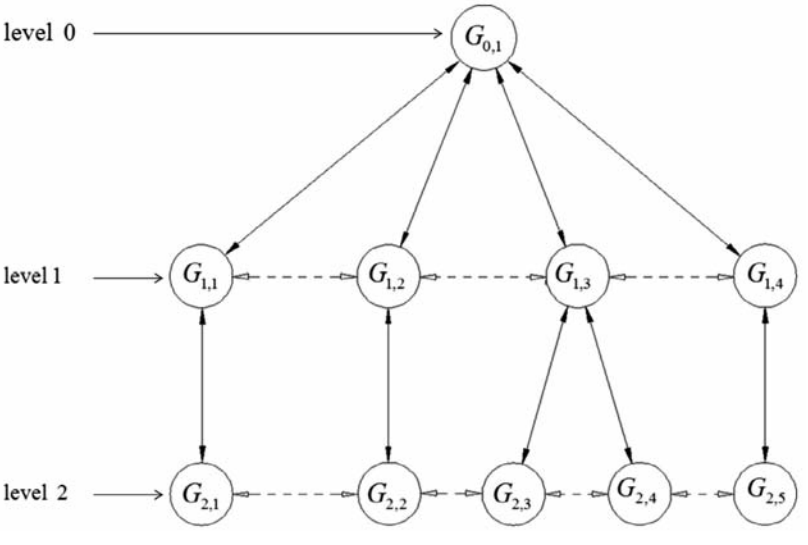

Fig. 2. 2D adaptive mesh of Berger-Oliger AMR Scheme. The superscript s denotes the level and the position in the data structure. The neighbor grids are refined by a ratio of 2:1. (a) Adaptive grid nested in the 2D spatial domain. (b) 2D tree data structure.

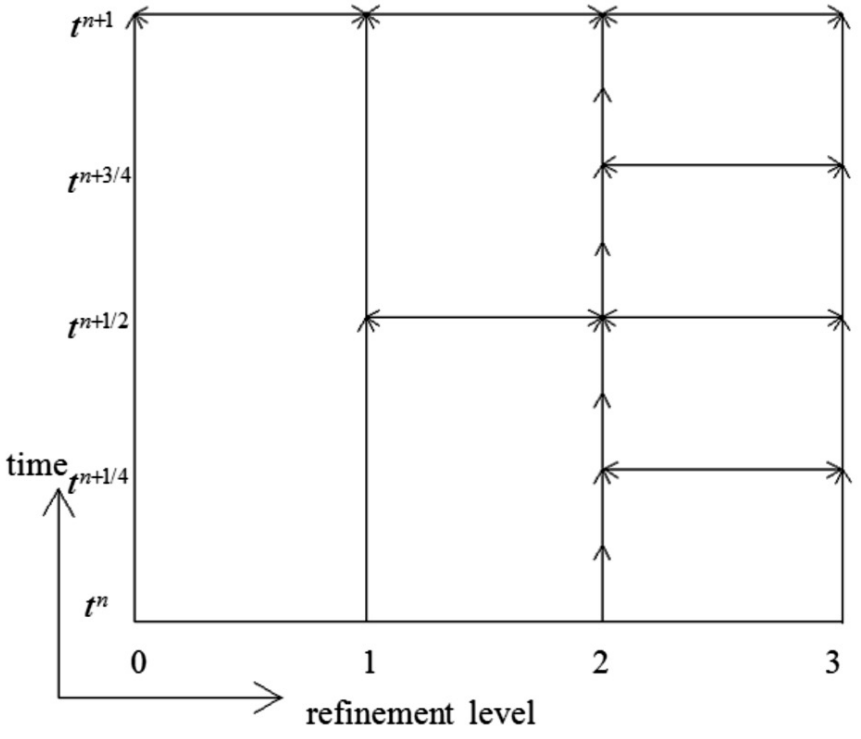

Fig. 3. Time step sequence during adaptive mesh refinement with refinement ratio equal to 2.

ERROR ESTIMATION

AMR algorithm generates adaptive mesh in which we need to estimate the error and adjust the grid structure at every time step. When a new fine grid is generated, its initial value is obtained by interpolating the existing solution (Berger, 1982; Berger and Oliger, 1984; Berger and Colella, 1989). We use the Richardson extrapolation estimation of the local truncation error (see Appendix A) to find the regions where the grid needs to be refined. It is a powerful numerical technique for improving the speed and accuracy in various mathematical methods.

The local truncation error is obtained by the Richardson extrapolation error estimation procedure. If the truncation error is greater than a given threshold value, the local rectangular region is refined. This is the criterium to construct the nested type of adaptive meshs. Although the Richardson extrapolation local truncation error estimation is more expensive from the computational point of view than the gradient detection, it can predict a larger error in the neighborhood of captured discontinuities.

DISCRETE ACOUSTIC WAVE EQUATION

One spatial dimension

In one spatial dimension, the acoustic wave equation is a variable coefficient linear hyperbolic system (LeVeque, 1997, 2002)

$$q_1 + A(x)q_x = 0 \quad , \tag{1}$$

where the coefficients matrices A(x) are given by

$$A(x) = \begin{bmatrix} 0 & K(x) \\ \rho^{-1}(x) & 0 \end{bmatrix} . \tag{2}$$

The coefficients matrices A(x) with their elements are determined by the density $\rho(x)$ and bulk modulus of elasticity K(x). The sound speed c(x) is defined by

$$c(x) = [K(x)/\rho(x)]^{1/2} \quad . \tag{3}$$

At the interface between any two cells x_{i-1} and x_i the Riemann condition for (1) given the piecewise constant initial data, is given by

$$q(x_i,0) = \begin{cases} q_{i-1} & x < x_{i-1/2} \\ q_i & x > x_{i-1/2} \end{cases} . \tag{4}$$

Let the value Q_i^n be a cell average over the uniform Cartesian x_i grid cell in two dimensions at the time t_n (Ketcheson and LeVeque, 2008)

$$Q_i^n \approx (1/\Delta x) \int_{x_{i-1/2}}^{x_{i+1/2}} q(x_i,t_n)dx \quad . \tag{5}$$

Two states Q_{i-1} and Q_i must be the sum of M_w waves $W_{i-1/2}^p$, defined by

$$\sum_{p=1}^{Mw} W_{i-1/2}^p = Q_i - Q_{i-1} \equiv \Delta Q_{i-1/2} \quad . \tag{6}$$

The Riemann solution has one left going wave $A^-\Delta Q_{i-1/2}$ and one right going wave $A^+\Delta Q_{i-1/2}$ at each interface. The fluctuations are given by

$$A^-\Delta Q_{i-1/2} + A^+\Delta Q_{i-1/2} = f(Q_i) - (Q_{i-1}) \quad . \tag{7}$$

For variable coefficient linear hyperbolic system of equation, the eigenvector matrices for A(x) can be expressed (LeVeque, 2002) by

$$A(x)q_x = f(q)_x \quad . \tag{8}$$

For eq. (7), the left and right going wave fluctuations can be defined by

$$\begin{aligned} A^-\Delta Q_{i-1/2} &= \sum_p (c^p_{i-1/2})^- W^p_{i-1/2} \quad , \\ A^+\Delta Q_{i-1/2} &= \sum_p (c^p_{i-1/2})^+ W^p_{i-1/2} \quad . \end{aligned} \tag{9}$$

We can obtain wave propagation from the fluctuations that are used for the Godunov method with one-order accuracy

$$Q^{n+1}_i = Q^n_i - (\Delta t/\Delta x)(A^+\Delta Q_{i-1/2} + A^-\Delta Q_{i+1/2}) \quad . \tag{10}$$

The Godunov method (10) adds correction terms for high-resolution methods to describe the waves and speeds by the Riemann solver, which has second-order accuracy (LeVeque, 1997, 2002; Ketcheson and LeVeque, 2008; Calhoun et al., 2008)

$$Q^{n+1}_i = Q^n_i - (\Delta t/\Delta x)(A^+\Delta Q_{i-1/2} + A^-\Delta Q_{i+1/2} + \tilde{F}_{i+1/2} - \tilde{F}_{i-1/2}) \quad , \tag{11}$$

where $\tilde{F}_{i\pm1/2}$ is the correction flux

$$\tilde{F}_{i\pm1/2} = \tfrac{1}{2} \sum_{p=1}^{Mw} |c^p_{i\pm1/2}|[1 - (\Delta t/\Delta x)|c^p_{i\pm1/2}|]\tilde{W}^p_{i-1/2} \quad , \tag{12}$$

and the wave $\tilde{W}^p_{i-1/2}$ is a limited version of $W^p_{i-1/2}$ to avoid oscillations (see Appendix B).

Two spatial dimensions

We consider the 2D first-order stress-velocity acoustic wave equation for wave propagation. The acoustic wave equation can be written

$$q_t + A(x,y)q_x + B(x,y)q_y = 0 \quad . \tag{13}$$

Here, the vector q consists of the pressure field p(x,y) and the velocities u(x,y) and v(x,y) can be written as

$$q = \begin{bmatrix} p \\ u \\ v \end{bmatrix} \quad , \tag{14}$$

$$A(x,y) = \begin{bmatrix} 0 & K(x,y) & 0 \\ \rho^{-1}(x,y) & 0 & 0 \\ 0 & 0 & 0 \end{bmatrix}, \tag{15}$$

$$B(x,y) = \begin{bmatrix} 0 & 0 & K(x,y) \\ 0 & 0 & 0 \\ \rho^{-1}(x,y) & 0 & 0 \end{bmatrix}. \tag{16}$$

The coefficients matrices A(x,y) and B(x,y) with their elements are determined by the density $\rho(x,y)$ and bulk modulus of elasticity K(x,y). The sound speed c(x,y) is defined once more by

$$c(x,y) = [K(x,y)/\rho(x,y)]^{1/2} . \tag{17}$$

We use the high-resolution methods to describe the waves and speeds by the Riemann solver, with a second-order accuracy (LeVeque, 1997, 2002; Ketcheson and LeVeque, 2008; Calhoun et al., 2008). The detailed process can be found in Appendix C.

$$Q^{n+1}_{i,j} = Q^{n}_{i,j} - (\Delta t/\Delta x)(A^{+}\Delta Q_{i-1/2,j} + A^{-}\Delta Q_{i+1/2,j} + \tilde{F}_{i+1/2,j} - \tilde{F}_{i-1/2,j}) - (\Delta t/\Delta y)(B^{+}\Delta Q_{i-1/2,j} + B^{-}\Delta Q_{i+1/2,j} + \tilde{G}_{i+1/2,j} - \tilde{G}_{i-1/2,j}) . \tag{18}$$

The numerical solutions of coarse mesh can be obtained from the formulation (18). One uses the coarse-level numerical solutions attaining the finer level numerical solutions on the adaptive meshes. The solutions of local rectangular patches of the finer level replace coarse mesh solutions, which are average of the finer meshes solutions. AMR algorithm adaptively generates local refinement mesh patches that update the solutions of the coarse meshes at every few time steps.

$$Q^{l+1}_{i,j} = Q^{l}_{i,j} - [(\Delta t/r^{l+1})/(\Delta x/r^{l+1})](\tilde{F}^{l}_{i+1/2,j} - \tilde{F}^{l}_{i-1/2,j}) - [(\Delta t/r^{l+1})/(\Delta y/r^{l+1})](G^{l}_{i,j+1/2} - G^{l}_{i,j-1/2}) , \quad l = 0,1,\ldots L \tag{19}$$

where l is the level, L is the largest level of the adaptive mesh, and r is the refinement ratio of the time steps of length to the space of width on the finer level.

In this paper, we use zero-order-extrapolation absorbing boundary conditions for numerical simulation of the 2D wave equation. Such absorbing conditions have proven to be very efficient for wave equation written as a first-order system in velocity and stress (LeVeque, 2002).

NUMERICAL EXPERIMENTS

In the first example, we consider wave propagation in a layered 2D homogeneous model. The coarse mesh is defined on a 320 × 320 grid with a space step of 4 m and time step of 2 ms. The wave velocity varies from 1100 to 1800 m/s (as shown in Fig. 4). The source coordinate is located at (x_0 = 640 m, y_0 = 640 m) in the upper part of the model, and two receivers are at R_1 (640,800) and R_2 (640,400). The threshold tolerance for the Richardson estimation of truncation error is 10^{-4}, and three levels mesh refinement grids are used. The size of stable time steps is determined by the CFL condition (Courant number equal to 0.9). The source function used in initial pressure as follows

$$f(x,y,t) = \sin(\pi r/a) \quad , \quad t = 0,\ r < a \tag{20}$$

$$f(x,y,t) = 0 \quad , \quad t = 0,\ r \geq a \tag{21}$$

$$r = 4\pi[\{(x-x_0) \times 10^{-3}\}^2 + \{(y-y_0) \times 10^{-3}\}^2]^{1/2} \quad . \quad t=0,\ r<a \tag{22}$$

Here, a = 0.1, a pressure source at the location (x_0,y_0).

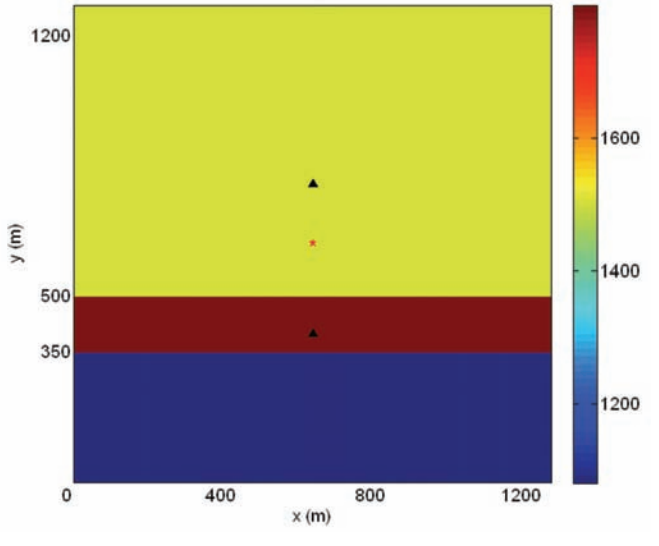

Fig. 4. The model of three-layer media.

In Fig. 5, every small rectangular border regions express locally rectangular finer mesh patches for different snapshots. At each interface, e.g., between t = 0.20 s and 0.30 s, part of the energy is reflected. Since the wave velocity in the second layer media is larger than the one in the first layer, the waveform turns wider; on the other hand, the waveform turns thinner in the third media. The wave is reflected several times and creates internal multiples. The wave energy is absorbed at the boundary condition at t = 0.64 s. We do not observe any numerical dispersion in the different snapshots.

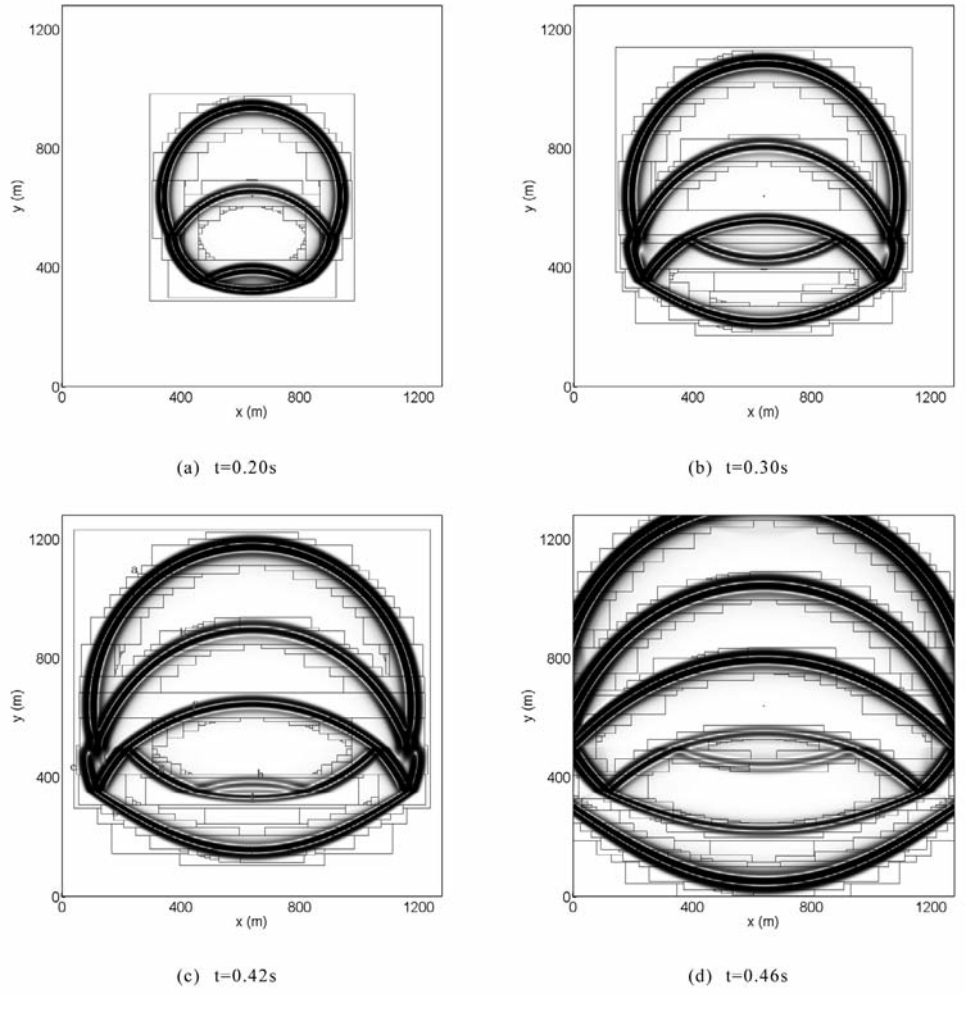

Fig. 5. Snapshots for different propagation times.

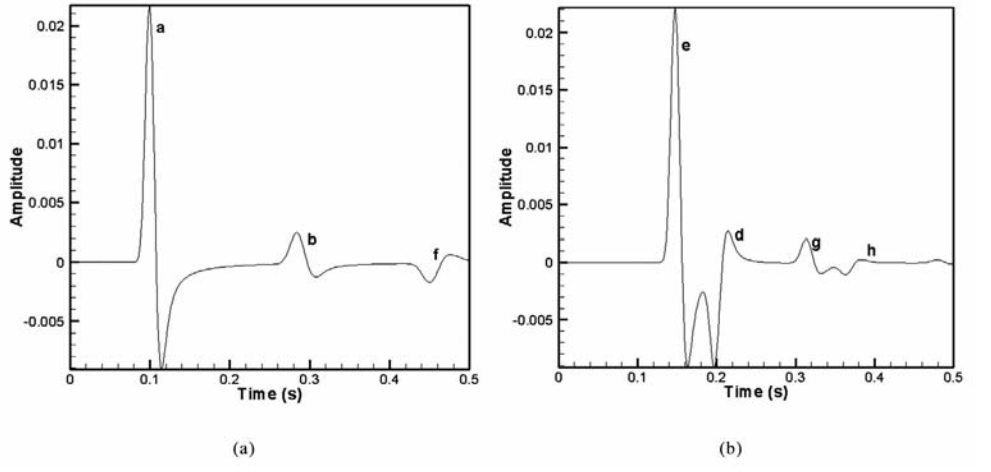

Fig. 6. The two receivers at $R_1(640,800)$ and $R_2(640,400)$.

In Fig. 6, the two receivers describe how wave energy changes with function of time. We do not observe numerical dispersion, because AMR can obtain high-resolution and smooth solution.

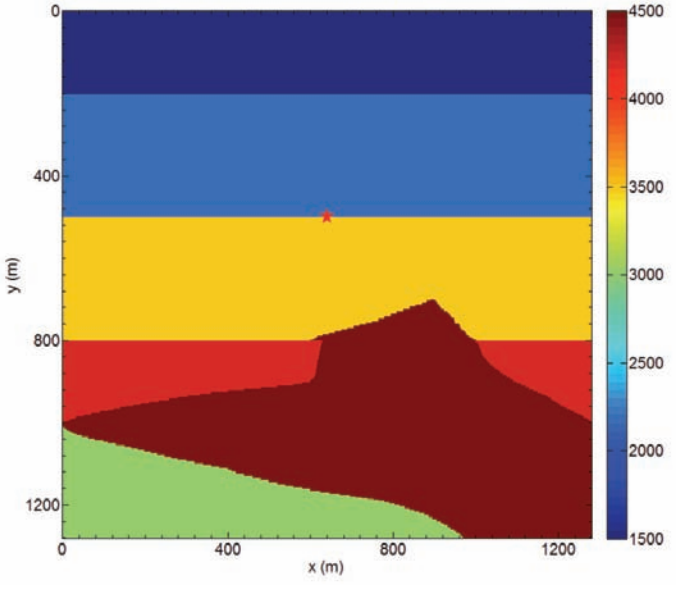

Fig. 7. The more complex velocity models, with velocity increasing with depth.

The second example deals with a more complex model to simulate the wave propagation through a salt body (as shown in Fig. 7). The model is discretized on a 256 by 256 grid with a distance of 5 m between two points. The time integration is 1 ms. The source coordinate is at (640 m,500 m). Threshold tolerance for the Richardson truncation error is 10^{-4}, and three levels mesh refinement grids are used.

In Fig. 7, velocities vary from 1500 to 4500 m/s. The region with the highest velocity was designed to simulate the wave propagation through a salt dome body. Diffracted energy and multiples can be observed on the different snapshots (Fig. 8).

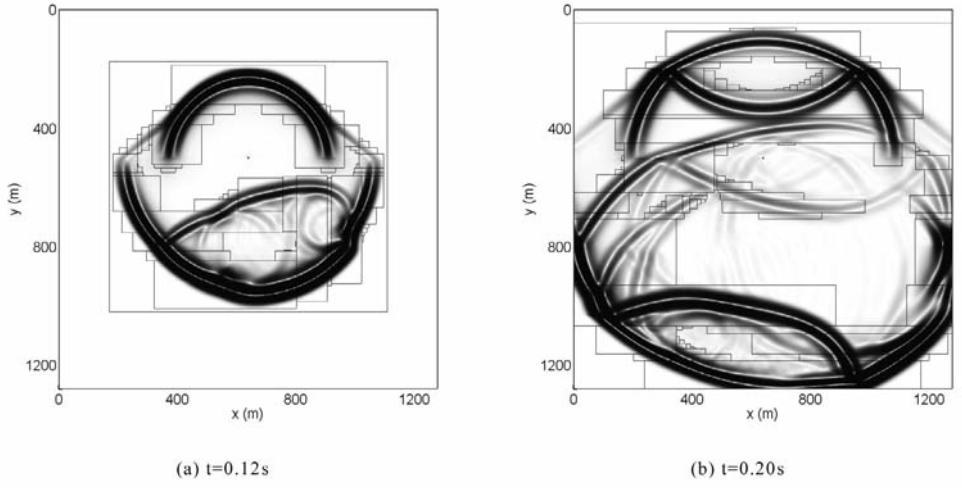

Fig. 8. The snapshot of wave propagation in complex media at different times.

We use a PC with 2 GB memory and the CPU AMD Phenom 9600. We take the model shown in Fig. 5 as example. In Fig. 9, the running time of the proposed AMR is much smaller than the one obtained by the finer mesh method. With increasing running time, the wave field becomes more and more complex and the AMR method needs more coefficients to correctly describe the wave field. The ratio of the running time between the AMR and fine-mesh high-resolution wave propagation algorithm is 0.048 at t = 0.06 s and grows up to 0.40 at t = 0.5 s. If we use the finest mesh that the total computational time is 1.64×10^4 s, on the other hand, we use adaptive mesh that the computational time is only 6.6×10^3 s. The proposed algorithm reduces the computational time while preserving high resolution. This is helpful for large-scale modeling of seismic wave propagation, especially in models iteratively built in a travel time tomography approach.

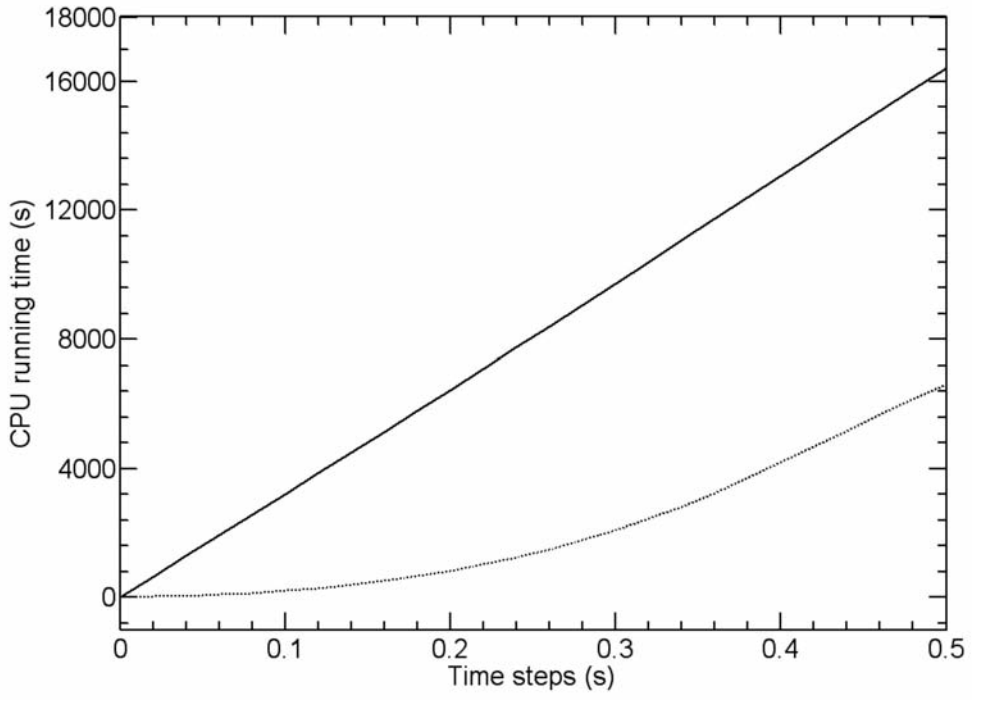

Fig. 9. Comparison of CPU running time between adaptive mesh (below dashed line) and finer mesh (above solid line) as the time steps increase. The horizontal coordinate denotes the maximum time for the wave propagation.

CONCLUSIONS

In this paper, we have presented an effective algorithm for numerical modeling of wave equations in layer media using adaptive mesh refinement. The method provides an accurate and efficient solution for wave propagation through the fine local rectangular patches. The fine reflection and transmission are properly modeled. By choosing appropriate thresholds, one can generate adaptive grids and controllable truncation errors. The proposed method is promising for the simulation of wave propagation in large-scale problems. We aim at applying this method in more complex models in the future. This AMR method can be also combined with wavelet transform or curvelet transform (Ma et al., 2007) to further improve the computational performance of seismic modeling.

ACKNOWLEDGMENTS

The authors would like to thank financial support from National Natural Science Foundation of China under grant number 10572072 and 40704019, National Basic Research Program of China (973 program) under grant number 2007CB209505.

REFERENCES

Barad, M. and Colella, P., 2005. A fourth-order accurate local refinement method for Possion's equation. J. Comput. Phys., 209: 1-18.

Berger, M., 1982. Adaptive Mesh Refinement for Hyperbolic Partial Differential Equations. Ph.D. Thesis, Stanford University.

Berger, M. and Oliger, J., 1984. Adaptive mesh refinement for hyperbolic partial differential equations. J. Comput. Phys., 53: 484-512.

Berger, M., 1986. Data structures for adaptive grid generation. SIAM J. Sci. Stat. Comput., 7: 904-916.

Berger, M. and Colella, P., 1989. Local adaptive mesh refinement for shock hydrodynamics. J. Comput. Phys., 82: 64-84.

Berger, M. and Rigoutsos, L., 1991. An algorithm for point clustering and grid generation. IEEE. T. Syst. Man. Cy., 21: 1278-1286.

Berger, M. and Leveque, R., 1998. Adaptive mesh refinement using wave-propagation algorithms for hyperbolic systems, SIAM J. Numer. Anal., 35: 2298-2316.

Bishop, T., Bube, K., Cutler, R., Langan, R., Love, P., Resnick, J., Shuey, R., Spindler, D. and Wyld, H., 1986. Tomographic determination of velocity and depth in laterally varying media. Geophysics, 50: 903-923.

Bolstad, J., 1982. An Adaptive Finite Difference Method for Hyperbolic Systems in One Space Dimension. Ph.D. Thesis, Stanford University.

Calhoun, D., Helzel, C. and LeVeque, R., 2008. Logically rectangular grids and finite volume methods for PDEs in circular and spherical domains. SIAM Review, 50: 723-752.

Debreu, L., Vouland, C. and Blayo, E., 2008. AGRIF: Adaptive grid refinement in Fortran. Comput. Geosci-UK, 34: 8-13.

Griebel, M. and Zumbusch, G., 1998. Adaptive space grids for hyperbolic conservation laws. Proc. of the 7th Internat. Conf. on Hyperbolic Problems, Basel, Switzerland.

Horning, R. and Trangenstein, J., 1997. Adaptive mesh refinement and multilevel iteration for flow in porous media, J. Comput. Phys., 136: 522-545.

Ketcheson, D. and LeVeque, R., 2008. WENOCLAW: A higher order wave propagation method, Hyperbolic Problem: Theory, Numerics, Applications. Springer Verlag, Berlin: 609-616.

Lanseth, J. and LeVeque, R., 2000. A wave propagation method for three-dimensional hyperbolic conservation laws. J. Comput. Phys., 165: 126-166.

LeVeque, R., 1997. Wave propagation algorithms for multidimensional hyperbolic systems. J. Comput. Phys., 131: 327-353.

LeVeque, R., 2002. Finite volume methods for hyperbolic problems. Cambridge University Press, Cambridge.

Ma, J., Gang, T. and Hussaini, M.Y., 2007. A refining estimation for adaptive solution of wave equation based on curvelets. In: Van De Ville, V., Goyal, K. and Papadakis, M. (Eds.), Wavelets XII, Proc. SPIE Vol. 6701, 67012J.

Mi, T. Ma, J. and Yang, H., 2009. Adaptive grid simulation of wave equations based on second generation wavelet transform. Submitted to Geophysics.

Mitra, S., Parashar, M. and Browne, J., 1997. DAGH: User's Guide, Dept. of Computer Sciences. Univ. of Texas at Austin. http://www.caip.rutgers.edu/~parashar/DAGH/

Pancheshnyi, S. Segur, P., Capeilere, J. and Bourdon, A., 2008. Numercial simulation of filamentary discharges with parallel adaptive mesh refinement. J. Comput. Phys., 227: 6574-6590.

Qian, J. and Symes, W., 2002. An adaptive finite-difference method for traveltimes and amplitudes. Geophysics, 67: 167-176.

Trangenstein, J., 1995. Adaptive mesh refinement for wave propagation in nonlinear solid. SIAM J. Sci. Comput., 16: 819-839.

APPENDIX A

In this appendix, we introduce the Richardson extrapolation estimates for the local truncation error, in order to get the finer mesh on each level (Berger, 1982; Berger and Oliger, 1984; Berger and Colella, 1989). We assume that the difference operator L has an order accuracy in both time and space domains, and then compare our numerical solutions. If a given solution Q(x,t) is very accurate, the local truncation error can be expressed

$$\begin{aligned} Q(x,t+k) &= LQ(x,t) + k[k''a(x,t) + h''b(x,t)] + kO[k^{n+1} + h^{n+1}] \\ &= \tau + kO[k^{n+1} + h^{n+1}] \quad , \end{aligned} \tag{A-1}$$

where the leading term is denoted by τ. If Q(x,t) is very accurate, then we use double time steps and double space widths with the difference operator L. Then

$$Q(x,t+2k) = L^2Q(x,t) + 2\tau + kO[k^{n+1} + h^{n+1}] \quad , \tag{A-2}$$

$$\begin{aligned} Q(x,t+2k) &= L_{2h}Q(x,t) + (2k)[(2k)''a(x,t) + (2h)''b(x,t)] + O[h^{n+2}] \\ &= 2^{n+1}\tau + kO[h^{n+2}] \quad , \end{aligned} \tag{A-3}$$

where the error order is of 2τ

$$Q[x,t+2k - L^2Q(x,t)] \approx 2\tau \quad . \tag{A-4}$$

Taking formula (A-2) and (A-3) with the integration scheme, one can get the local truncation error at time t.

$$[L^2Q(x,t) - L_{2h}Q(x,t)]/(2^{n+1} - 2) = \tau + O(h^{n+2}) \quad . \tag{A-5}$$

Using the Richardson extrapolation error estimation, the solution is propagated in time in two different ways for finding the refinement regions. The first occurs on the fine level, and the second occurs on coarse level, and then compares two solutions to determine where grids need some refinement.

APPENDIX B

In this appendix, we present expressions for the wave $\tilde{W}^p_{i-1/2}$ being a limited version of $W^p_{i-1/2}$ to avoid oscillations. Wave limiters can obtain high resolution wave propagation and reduce numerical oscillations (LeVeque, 1997). For the 1D acoustic eq. (1) one can obtain

$$W^p_i = \alpha^p_i r^p \quad , \tag{B-1}$$

where α^p_i is a scalar. Note that the vector r^p is independent of i. The flux limiter replaces each wave W^p_i by a limited version

$$\tilde{W}^p_i = \varphi(\theta^p_i) W^p_i \quad . \tag{B-2}$$

Here θ^p_i is some measure of smoothness of the solution given by

$$\theta^p_i = (W^p_{i-1} \cdot W^p_i)/(W^p_i \cdot W^p_i) \quad . \tag{B-3}$$

There are some standard limiters (LeVeque, 1997)

minmod: $$\varphi(\theta) = \max[0,\min(1,\theta)] \quad , \tag{B-4a}$$

superbee: $$\varphi(\theta) = \max[0,\min(1,2\theta),\min(2,\theta)] \quad , \tag{B-4b}$$

monotonized centered: $$\varphi(\theta) = \max(0,[\min(1+\theta)/2,2,2\theta]) \quad . \tag{B-4c}$$

We can choose the standard limiters based on the problem. Minmod limiter is the most diffusive limiter that chooses the wave with the smallest of the two compared in the same direction. Superbee limiter is applied to discontinuities solution. Monotonized centered limiter is good choice for most problems (Lanseth and LeVeque, 2000).

APPENDIX C

In this appendix, we present expressions for the second-order accuracy high-resolution methods (18). Let the value $Q^n_{i,j}$ represent a cell average over the uniform Cartesian (i,j) grid cell in two dimensions at the time t_n

$$Q^n_{i,j} \approx (1/\Delta x \Delta y) \int_{y_{j-1/2}}^{y_{j+1/2}} \int_{x_{i-1/2}}^{x_{i+1/2}} q(x,y,t_n) dx dy \quad . \tag{C-1}$$

For variable coefficient linear hyperbolic system of equation, the eigenvector matrices for A(x,y) and B(x,y) can be expressed as

$$A(x,y)q = f(q), \quad B(x,y)q = g(q) \quad . \tag{C-2}$$

We use high-resolution wave propagation algorithm for the simulation of the 2D acoustic wave eq. (13) (LeVeque, 1997, 2002; Ketcheson and LeVeque, 2008; Calhoun et al., 2008)

$$\begin{aligned} Q^{n+1}_{i,j} = Q^{n}_{i,j} &- (\Delta t/\Delta x)[\sum_{p=1}^{Mw} (c^{p}_{i-1/2,j})^{+} W^{p}_{i-1/2,j} + \sum_{p=1}^{Mw} (c^{p}_{i+1/2,j})^{-} W^{p}_{i+1/2,j}] \\ &- (\Delta t/\Delta y)[\sum_{p=1}^{Mw} (c^{p}_{i,j-1/2})^{+} W^{p}_{i,j-1/2} + \sum_{p=1}^{Mw} (c^{p}_{i,j+1/2})^{-} W^{p}_{i,j+1/2}] \\ &- (\Delta t/\Delta x)[\tilde{F}_{i+1/2,j} - \tilde{F}_{i-1/2,j}] - (\Delta t/\Delta y)[\tilde{G}_{i,j+1/2} - \tilde{G}_{i,j-1/2}] \quad . \end{aligned} \tag{C-3}$$

Here, $Q_{i,j}$ denote the cell average of q over the i-th and j-th cells in the grid, with the correction fluxes $\tilde{F}$ for wave propagation in the x-direction, and the correction fluxes $\tilde{G}$ in the y-direction defined by

$$\begin{aligned} \tilde{F}_{i+1/2,j} &= \tfrac{1}{2} \sum_{p=1}^{Mw} |c^{p}_{i+1/2,j}|[1 - (\Delta t/\Delta x)|c^{p}_{i+1/2,j}|]\tilde{W}^{p}_{i+1/2,j} \quad , \\ \tilde{F}_{i-1/2,j} &= \tfrac{1}{2} \sum_{p=1}^{Mw} |c^{p}_{i-1/2,j}|[1 - (\Delta t/\Delta x)|c^{p}_{i-1/2,j}|]\tilde{W}^{p}_{i-1/2,j} \quad , \\ \tilde{G}_{i,j+1/2} &= \tfrac{1}{2} \sum_{p=1}^{Mw} |c^{p}_{i,j+1/2}|[1 - (\Delta t/\Delta x)|c^{p}_{i,j+1/2}|]\tilde{W}^{p}_{i,j+1/2} \quad , \\ \tilde{G}_{i,j-1/2} &= \tfrac{1}{2} \sum_{p=1}^{Mw} |c^{p}_{i,j-1/2}|[1 - (\Delta t/\Delta x)|c^{p}_{i,j-1/2}|]\tilde{W}^{p}_{i,j-1/2} \quad . \end{aligned} \tag{C-4}$$

Here, the wave $\tilde{W}$ is a limited version of W to avoid oscillations. The waves $\tilde{W}^{p}_{i-1/2,j}$ and $\tilde{W}^{p}_{i+1/2,j}$ are Riemann problems solutions in the x-direction at the interfaces, and $\tilde{W}^{p}_{i,j-1/2}$ and $\tilde{W}^{p}_{i,j+1/2}$ are Riemann problems solution in the y-direction at the interfaces.

In formulation (C-4), a set of Mw waves W and speeds c can be written as (Ketcheson and LeVeque, 2008)

$$
\begin{aligned}
\sum_{p=1}^{Mw} W^{p}_{i-1/2,j} &= Q_{i,j} - Q_{i-1,j} \equiv \Delta Q_{i-1/2,j} \quad , \\
\sum_{p=1}^{Mw} W^{p}_{i+1/2,j} &= Q_{i+1,j} - Q_{i,j} \equiv \Delta Q_{i+1/2,j} \quad , \\
\sum_{p=1}^{Mw} W^{p}_{i,j-1/2} &= Q_{i,j} - Q_{i,j-1} \equiv \Delta Q_{i,j-1/2} \quad , \\
\sum_{p=1}^{Mw} W^{p}_{i,j+1/2} &= Q_{i,j+1} - Q_{i,j} \equiv \Delta Q_{i,j+1/2} \quad .
\end{aligned}
\tag{C-5}
$$

The standard conservation law can be expressed by

$$
\begin{aligned}
A^{-}\Delta Q_{i-1/2,j} + A^{+}\Delta Q_{i-1/2,j} &= f(Q_{i,j}) - f(Q_{i-1,j}) \quad , \\
A^{-}\Delta Q_{i+1/2,j} + A^{+}\Delta Q_{i+1/2,j} &= f(Q_{i+1,j}) - f(Q_{i,j}) \quad , \\
B^{-}\Delta Q_{i,j-1/2} + B^{+}\Delta Q_{i,j-1/2} &= g(Q_{i,j}) - g(Q_{i,j-1}) \quad , \\
B^{-}\Delta Q_{i,j+1/2} + B^{+}\Delta Q_{i,j+1/2} &= g(Q_{i,j+1}) - g(Q_{i,j}) \quad .
\end{aligned}
\tag{C-6}
$$

The Riemann solutions are defined in terms of the right-going fluctuation $A^{+}\Delta Q_{i\mp1/2,j}$ at the left edge of cell i, while the left-going fluctuation $A^{-}\Delta Q_{i\mp1/2,j}$ at the right edge of this cell in the x-direction, and fluctuations $B^{+}\Delta Q_{i,j\mp1/2}$ and $B^{-}\Delta Q_{i,j\mp1/2}$ in the y-direction.

$$
\begin{aligned}
A^{\pm}\Delta Q_{i-1/2,j} &= \sum_{p} (c^{p}_{i-1/2,j})^{\pm} W^{p}_{i-1/2,j} \quad , \\
A^{\pm}\Delta Q_{i+1/2,j} &= \sum_{p} (c^{p}_{i+1/2,j})^{\pm} W^{p}_{i+1/2,j} \quad , \\
B^{\pm}\Delta Q_{i,j-1/2} &= \sum_{p} (c^{p}_{i,j-1/2})^{\pm} W^{p}_{i,j-1/2} \quad , \\
B^{\pm}\Delta Q_{i,j+1/2} &= \sum_{p} (c^{p}_{i,j+1/2})^{\pm} W^{p}_{i,j+1/2} \quad .
\end{aligned}
\tag{C-7}
$$